Proceedings of the Seventh International Conference on
Railway Technology: Research, Development and Maintenance
Edited by: J. Pombo
Civil-Comp Conferences, Volume 15, Paper 5.10
Civil-Comp Press, Edinburgh, United Kingdom, 2026
ISSN: 2753-3239, doi: 10.4203/ccc.15.5.10
©Civil-Comp Ltd, Edinburgh, UK, 2026

Aerodynamic Forces in Intermodal Container Trains: A Study on the Effect of Wagon Position on Container Drag

L. Corniani[1], P. Schito[1], J. R. Bell[2], J. Pombo[3] and S. Bruni[1]

[1]**Department of Mechanical Engineering, Politecnico di Milano, Italy**
[2]**Institute of Aerodynamics and Flow Technology, German Aerospace Center e.V., Göttingen, Germany**
[3]**Institute of Railway Research, University of Huddersfield, United Kingdom**

Abstract

Aerodynamic forces have a crucial role in the safe and efficient operation of freight trains. In particular, the drag of intermodal container trains is the focus of a considerable research effort because of its direct impact on the energy consumption and greenhouse gasses emissions of these the freight rail sector. The drag of containers in an intermodal container train can be affected by the proximity to the extremes of the train, among other factors. This means that the results obtained on one container train cannot be safely generalized to the other containers in a long intermodal container train, unless independence from these effects is established.
Numerical simulations have been run on train consists of different length to assess the minimum number of wagons necessary to ensure independence form proximity to the extremes of the train. The drag coefficients on the containers are presented, demonstrating that at least nine wagons should be simulated to achieve this condition for the fourth and fifth wagon.

Keywords: train aerodynamics, freight trains, CFD, RANS, drag, container position.

1 Introduction

The European Union (EU) has committed to reducing greenhouse gas emissions by 20% with respect to 2008 levels by 2030, with even more ambitious goals for 2050 [1]. For this reason, the EU plans to shift at least 30% of the road-transported freight to rail or waterways by 2030 [1]. Freight trains are the least carbon emitting mode of freight transportation on land [2], [3], however, in 2023 only 16.4% (by tonne·km) of the goods transported in the EU were transported on rail [4]. Despite the low emissions of freight trains, efficiency can still be significantly improved. Aerodynamic effects contribute substantially to the energy consumption of intermodal container trains (ICTs), especially with aerodynamically poor train compositions [5], [6]. The drag on each container depends on several factors, including its position on the train [7]. These effects however affect only a modest number of wagons. This means that for long ICTs most of the containers will be subject to "mid-train" conditions and experience a similar drag [8]. Computational Fluid Dynamics (CFD) is often employed to investigate the aerodynamics of freight trains (see reference [9] for an overview), but the computational cost of this tool grows rapidly with the number of wagons included, because more cells are be needed to carry out the simulation. This work employs CFD simulations to investigate the minimum number wagons that need to be added behind a locomotive to obtain values of drag independent of nose or tail effects.

Drag is directly related to energy consumption and is among the most frequent topic of investigation in freight train aerodynamics [9]. The container drag in ICTs depends on several factors beyond the container position on the train, such as inter-container gap [5], [6], [10], [11], [12] and yaw angle [13], [14], [15]. Scientific works have consistently found that larger gaps have the effect of increasing the drag on containers both downstream and upstream of the gap [5], [10]. This occurs because when the gaps are small the inter-container vortices prevent the flow form impinging in the gap, causing the containers to behave similarly to a single body [6]. When crosswind is present, the flow will enter the inter-container region, thus causing a higher drag for the same inter-container gap [13], [14]. It should also be noted that in the presence of crosswind, other aerodynamic forces (side force and lift) become relevant, as they may cause derailment or overturning if not managed properly [16]. The effect of container position in the train on drag has been observed in previous works [7], [17], [18] but is not yet completely understood. A numerical and experimental study proposed that 8 wagons in the wake of a locomotive are sufficient to produce drag on the fourth and fifth wagon independent of the effects on the extremes [17]. However, full-scale measurements [18] have obtained values of drag approximately 50% lower than comparable wind-tunnel experiments [6] and numerical works [19]. The greater distance from the nose was proposed as the main explanation for the discrepancy [18].

In this work, CFD simulations are run on different ICTs composed of a locomotive followed by 6, 7, 8 and 9 wagons. The drag coefficients on the containers placed on the wagons are then used to assess how many wagons are needed to obtain values of drag independent from the proximity of the container to the nose or tail of the train (from hereafter referred to as 'mid-train' conditions). This also makes a distinguishable contribution to the current body of knowledge by proposing this analysis on 60-ft wagons, with two containers mounted on each wagon in one of the possible real-service configurations.

2 Methods

In this work, CFD simulations have been run on freight trains composed of one locomotive and a variable number of 60-ft-wagons to assess the minimum number of wagons necessary to obtain "mid-train conditions". Train compositions with six, seven, eight and nine wagons were tested. On each 60-ft-wagon, two standard ISO 20-ft-containers were mounted, as shown in Figure 1b, the complete geometry of the 7-wagons train consist is shown in Figure 1a. The geometry of the locomotive and the wagons were taken from an open geometry database of freight rail vehicles [7], [20], [21].

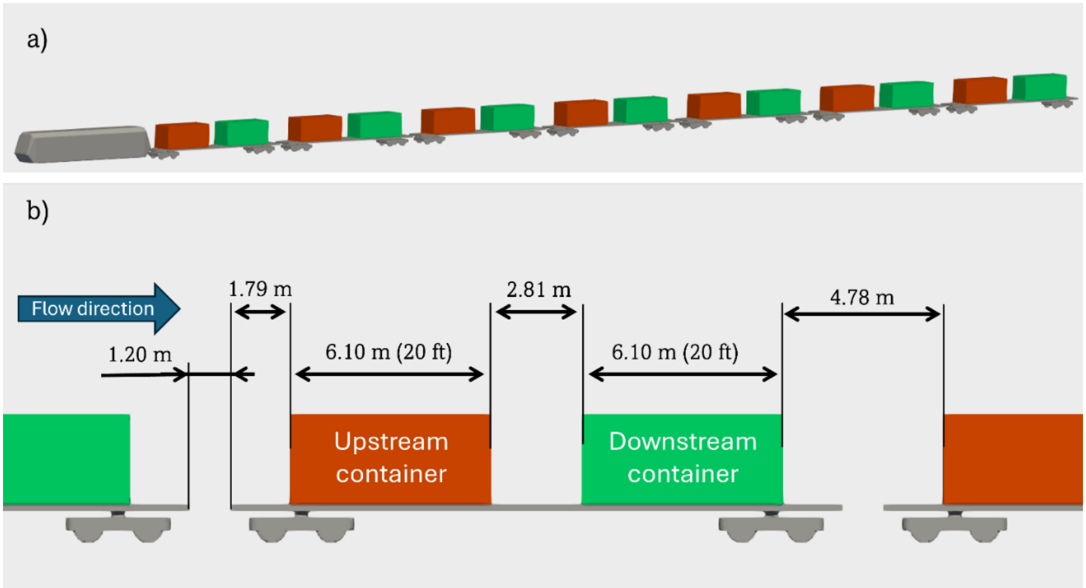

Figure 1. (a) 7-wagons train consist; (b) Dimensions of the gaps between containers and between wagons

It should be noted that the distance between wagons, as well as the position of containers on the wagons correspond to real-service positions.

The numerical simulations were run on the software openFoam, using a stationary Reynolds Averaged Navier Stokes (RANS) solver and modelling the turbulence with the k-omega Shear Stress Transport (k-ω SST) model. The suitability of the numerical methodology in terms independence from mesh dimensions and refinements was demonstrated in previous numerical campaigns. On all train surfaces, no-slip conditions were applied for velocity, and wall functions were adopted for turbulent kinetic energy (k), specific dissipation rate (ω) and turbulent viscosity (ν_T). On the inlet a uniform velocity field was set, with magnitude velocity of 120 km/h (resulting in a width-based Reynolds number of approximately 5.3 million). A zero-gradient condition was chosen for the pressure. The value of pressure was set to at the outlet, and on the other patches (including the ground) a no-slip condition was applied, together with zero-gradient for the pressure. The SIMPLE algorithm was used as a time-marching scheme, with one iteration of non-orthogonal correction. Space and time discretization were carried out with second-order schemes.

The forces were computed on every container at each iteration. After the simulations, the average drag coefficient ($\overline{C_D}$) on each container was computed with equation (1), using the standard value of 10 m^2 as a reference area (A_{REF}).

$$\overline{C_D} = \frac{\overline{F_D}}{\frac{1}{2}\rho U_{FS}^2 A_{REF}} \quad (1)$$

where $\overline{F_D}$ is the average drag force, ρ is the air density (assumed constant in the incompressible solver used in this work) and U_{FS} is the freestream velocity magnitude (equal to 33.33 m/s). The values of the average drag coefficient of the containers are reported and discussed in the next section.

3 Results and discussion

Drag coefficients on each container have been computed and recorded at each iteration of the simulation, and then an average value of the drag coefficient has been computed for each container. Table 1 shows the drag coefficient on every container in all the simulations run.

Wagon position	Container position	Average drag coefficient			
		6-wagons train consist	7-wagons train consist	8-wagons train consist	9-wagons train consist
Wagon 1	Upstream	0.292	0.331	0.269	0.318
Wagon 1	Downstream	0.149	0.153	0.124	0.128
Wagon 2	Upstream	0.213	0.216	0.104	0.110
Wagon 2	Downstream	0.155	0.160	0.142	0.124
Wagon 3	Upstream	0.208	0.198	0.174	0.179
Wagon 3	Downstream	0.123	0.127	0.151	0.132
Wagon 4	Upstream	0.178	0.192	0.181	0.183
Wagon 4	Downstream	0.122	0.117	0.119	0.132
Wagon 5	Upstream	0.194	0.168	0.186	0.184
Wagon 5	Downstream	0.126	0.133	0.102	0.133
Wagon 6	Upstream	0.187	0.183	0.188	0.185
Wagon 6	Downstream	0.154	0.117	0.122	0.123
Wagon 7	Upstream	-	0.201	0.202	0.207
Wagon 7	Downstream	-	0.165	0.140	0.112
Wagon 8	Upstream	-	-	0.177	0.185
Wagon 8	Downstream	-	-	0.144	0.124
Wagon 9	Upstream	-	-	-	0.200
Wagon 9	Downstream	-	-	-	0.181

Table 1. Average drag coefficients on all containers in the tested train consists

It can be observed in the results in Table 1 that containers mounted in the upstream position of the wagons exhibit larger $\overline{C_D}$ values than the ones mounted on the downstream position of the wagon. This is likely explained by the different upstream and downstream inter-container gaps and by the presence or absence of the wagon plane in the inter-container region. Because of these differences, it is useful to compare against each other the average drag coefficients of containers mounted in the upstream position of their respective wagons (upstream containers). In Figure 2 are plotted the values of $\overline{C_D}$ of the upstream containers in all train configurations.

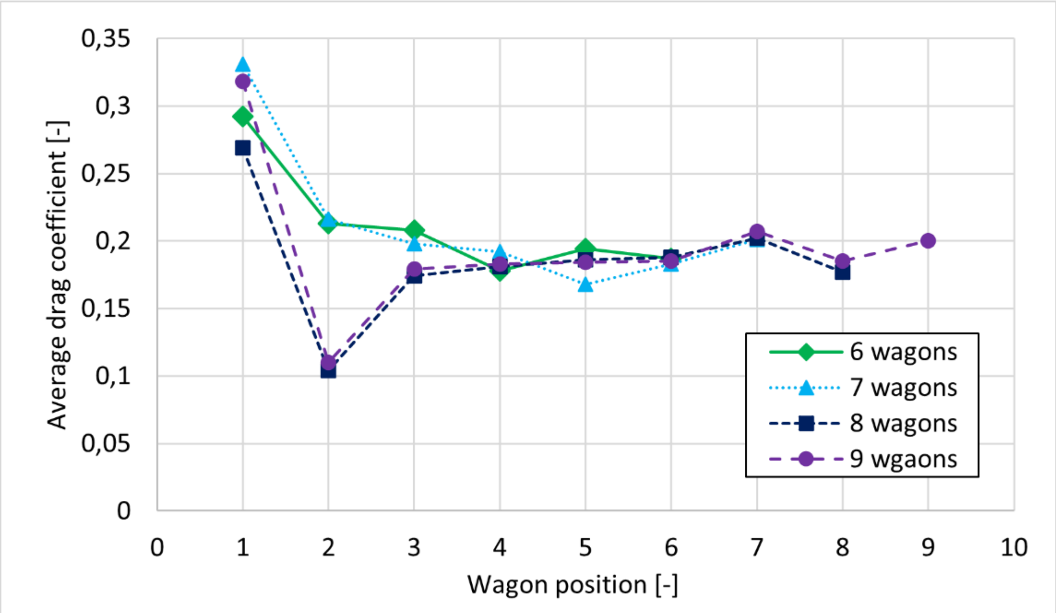

Figure 2. Average drag coefficients on upstream containers in all tested train compositions

Based on the results in Figure 2, the 6-wagons and 7-wagons train consists don't seem to reach a stable value of $\overline{C_D}$ for the upstream containers. The 8-wagons and 9-wagons train consists instead show a rather stable value of $\overline{C_D}$ for the containers on wagons 4 to 6. Additionally, the values of $\overline{C_D}$ for these wagons are extremely similar between the last two train consists, suggesting that the $\overline{C_D}$ on these containers are not dependent on the effects of proximity to the nose or tail of the train.

Similarly to the $\overline{C_D}$ values of the upstream containers, it is useful to make a separate comparison of the values of $\overline{C_D}$ on the downstream containers. Figure 3 shows the values of average drag coefficients on the downstream containers of all train consists.

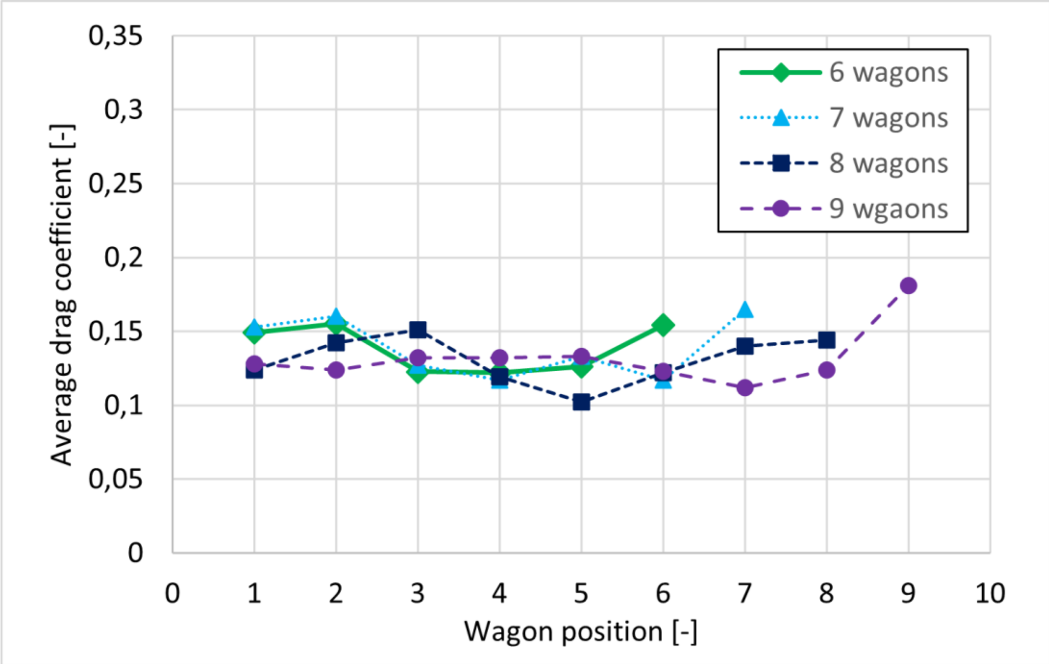

Figure 3. Average drag coefficients on downstream containers in all tested train compositions

It can be observed that the drag coefficients on downstream containers do not reach a stable value for any of the tested cases, except the 9-wagons train consist. In the 9-wagons train consist the $\overline{C_D}$ values for the containers on the wagons from 3 to 5 undergo extremely small changes and may be considered independent from the proximity to head and tail of the train.

From the separate comparisons of upstream and downstream containers, it can be concluded that the wagons 4 and 5 in a 9-wagons train consist are in mid-train conditions. On these wagons, the drag coefficients of all containers are independent from proximity effects form the extremes of the train. This finding does not imply that mid-train conditions on the containers of a single wagon may obtained with a shorter train, because a stable $\overline{C_D}$ value for downstream containers was not reached in the 8-wagons train consists.

Some similarities between all train compositions can be observed in Figure 2. The upstream container positioned on the first wagon is subject to the largest drag coefficient of all wagons in all the tested consists. This finding is consistent with previous CFD analyses run on comparable train consists [7]. This larger values of drag coefficients are in part explained by the proximity of the container to the train nose. Another reason identified in previous works, however, is the different shape of locomotive tail. This difference in geometry causes the flow to behave differently, as evidenced by the different pressure distribution that can be observed on the front face of the first container downstream of the locomotive.

The pressure coefficient is defined in equation (2) to enable a better comparison between different cases.

$$\overline{C_p} = \frac{\bar{p} - p_{FS}}{\frac{1}{2}\rho U_{FS}^2} \tag{2}$$

Where $\bar{p}$ is the average static pressure and p_{FS} is the freestream pressure (set to zero in this case). Figure 4 shows a comparison of the pressure coefficient distribution on the front face of different containers. Specifically, the $\overline{C_p}$ distribution on the upstream container from the present work (Figure 4a) and from the first container downstream of the locomotive from a previous comparable analysis [7] (Figure 4b). In contrast Figure 4c, Figure 4d, Figure 4e and Figure 4f show respectively the $\overline{C_p}$ distribution on the front face of the fourth, fifth, sixth and seventh upstream containers in the 9-wagons train composition.

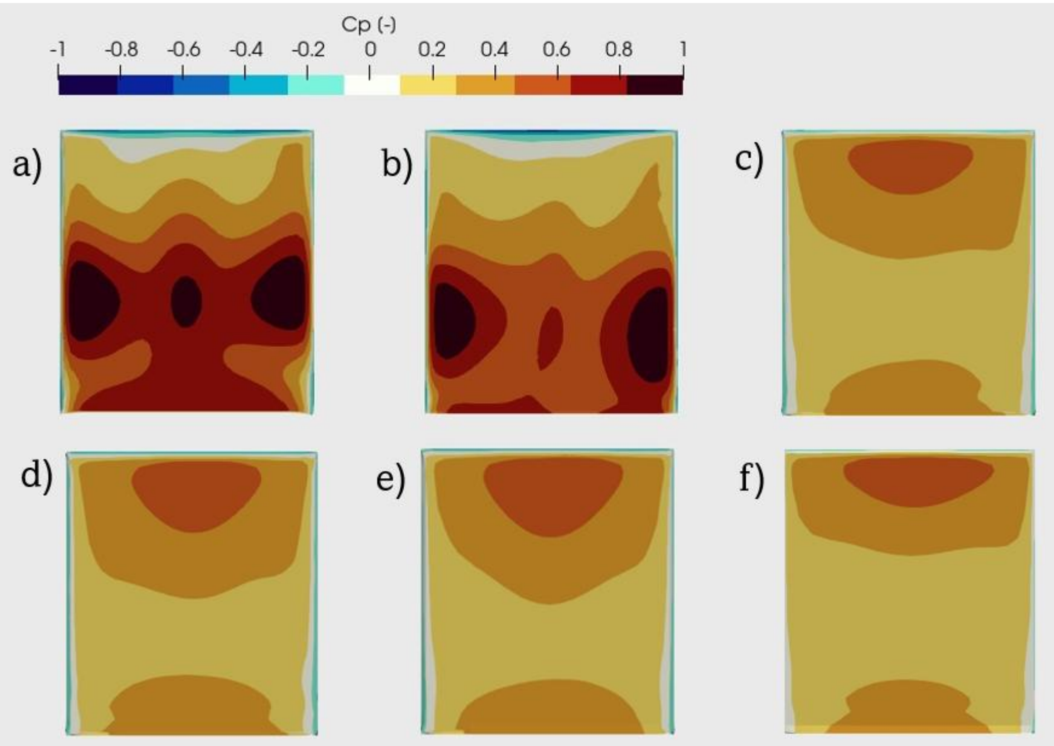

Figure 4. Average pressure coefficient distribution on: (a) the upstream container in wagon 1 of the 9-wagons train consist; (b) on the first container downstream of the locomotive in a previous analysis [7]; (c) the upstream container in wagon 4 of the 9-wagons

It can be observed that both in the present and previous study, the container immediately downstream of the locomotives presents a large high-pressure region roughly in the lower half of the container face, with regions of lower pressure at the top half. A different distribution is observed in Figure 4c to Figure 4f, where the highest-pressure region is on top and regions of lower pressure are at the medium height of the container face. These latter figures show that the pressure coefficient distribution in the 9-wagons train consist remain quite consistent for the upstream containers on these wagons.

The results in this study are compatible with previous work that analysed train consists composed of a locomotive followed by an increasing number of wagons [17]. This previous work suggested that a minimum number of eight wagons (behind a locomotive) were necessary to obtain aerodynamic forces on the fourth and fifth wagon that would be independent from proximity to the extremes. This previous study adopted some importantly different decisions (namely, the use of open wagons instead of couples of containers on flat wagons). Despite this difference, the results of this study are in broad agreement with the findings of the present work regarding upstream containers, while larger discrepancies exist with the findings of the present work regarding the downstream containers. This suggests aerodynamic forces on downstream containers are more sensitive to proximity to the extremes of the train than those on upstream containers.

4 Conclusions and Contributions

This work presents an investigation on the effects that the wagon position in a train consist has on the aerodynamic forces on containers. Specifically, a series of CFD simulations has been run on four train consists composed of an increasing number of wagons with containers mounted on them in real-service positions. The drag coefficients of the containers have been compared to assess the effect of proximity of the container to the nose or tail of the train, as well as the minimum number of wagons necessary to obtain container drag coefficients independent from these effects. A distinguishing contribution of this work is the fact that this analysis has been carried out on 60-ft containers, able to carry two 20-ft containers (in one of the possible real-service configuration). Separate investigation of drag coefficient behaviour in upstream/downstream containers were possible as a result of this choice.

The results of this work suggest that in simulating an intermodal freight train with the objective of determining aerodynamic forces on the containers, at least nine wagons should be included downstream of the locomotive for the results are to be independent of proximity effects from the nose and tail of the train. The simulations run on the 9-wagons train consist show that average drag coefficients on the containers mounted on the fourth and fifth wagons are not dependent on the proximity to the extremes of the train and could be considered representative for a long ICT.

The simulations of this work have been set up with freestream flow parallel to the longitudinal direction of the train (meaning with a yaw angle of 0 degrees). However, the presence of crosswind could carry the complex flow around each wagon away from the wagons downstream. This could potentially reduce the effect of the wake and thus change the minimum number of wagons needed to obtain mid-train conditions. Further research is needed to investigate the impact of crosswind on this point. Finally, this work is focused only on the drag coefficient of containers, but energy consumption of intermodal freight trains is dependent on the total drag of the wagons. Future research on this topic should also include the behaviour of drag coefficient of full wagons.

Acknowledgements

Funded by the European Union. Views and opinion expressed are however those of the author(s) only and do not necessarily reflect those of the European Union or the Europe's Rail Joint Undertaking. Neither the European Union nor the granting authority can be held responsible for them. The project Academics4Rail is supported by the Europe's Rail Joint Undertaking and its members.

References

[1] "White paper on transport – Roadmap to a single European transport area – Towards a competitive and resource efficient transport system," 2011. doi: 10.2832/30955.

[2] "Deutsche Bahn 2022 Integrated Report," 2022. Accessed: Feb. 06, 2026. [Online]. Available: https://ibir.deutschebahn.com/2022/en/home/

[3] "Seventh monitoring report on the development of the rail market," Brussels, Jan. 2021.

[4] "Statistical pocketbook 2025 - EU Transport in figures," Sep. 2025.

[5] A. Buhr, L. Siegel, J. Bell, and A. Henning, "Energy Savings for Freight Trains with Aerodynamically Optimized Loading Schemes," in *Proceedings of the Sixth International Conference on Railway Technology: Research, Development and Maintenance*, J. Pombo, Ed., Edinburgh: Civil-Comp Press, Sep. 2024. doi: 10.4203/ccc.7.3.2.

[6] C. Li, D. Burton, M. Kost, J. Sheridan, and M. C. Thompson, "Flow topology of a container train wagon subjected to varying local loading configurations," *Journal of Wind Engineering and Industrial Aerodynamics*, vol. 169, pp. 12–29, Oct. 2017, doi: 10.1016/j.jweia.2017.06.011.

[7] L. Corniani, P. Schito, J. R. Bell, J. Pombo, and S. Bruni, "Aerodynamics of Freight Trains – Addressing the Complexity of Train Geometry through an Open Database," *Promet - Traffic&Transportation*, vol. 38, no. 1, pp. 58–70, Jan. 2026, doi: 10.7307/ptt.v38i1.3096.

[8] Y.-C. Lai and C. P. L Barkan, "Options for Improving the Energy Efficiency of Intermodal Freight Trains," *Transportation Research Record: Journal of the Transportation Research Board*, pp. 47–55, 2005, doi: https://doi.org/10.1177/0361198105191600108.

[9] L. Corniani, P. Schito, J. Bell, and S. Bruni, "A review of freight train aerodynamics," *Proc. Inst. Mech. Eng. F J. Rail Rapid Transit*, vol. 240, no. 2, pp. 133–150, Feb. 2026, doi: 10.1177/09544097251382265.
[10] L. Siegel, A. Buhr, J. Bell, and A. Henning, "Analysis of Flow Structures in Different Loading Gaps of Freight Trains," in *Proceedings of the Sixth International Conference on Railway Technology: Research, Development and Maintenance*, J. Pombo, Ed., Edinburgh, Sep. 2024. doi: 10.4203/ccc.7.3.1.
[11] S. Maleki, "Numerical Investigations into the Aerodynamics of Freight Trains," Monash University, 2019.
[12] S. Maleki, D. Burton, and M. C. Thompson, "Flow structure between freight train containers with implications for aerodynamic drag," *Journal of Wind Engineering and Industrial Aerodynamics*, vol. 188, pp. 194–206, May 2019, doi: 10.1016/j.jweia.2019.02.007.
[13] A. Quazi, T. Crouch, J. Bell, T. McGreevy, M. C. Thompson, and D. Burton, "A field study on the aerodynamics of freight trains," *Journal of Wind Engineering and Industrial Aerodynamics*, vol. 209, Feb. 2021, doi: 10.1016/j.jweia.2020.104463.
[14] S. Maleki, D. Burton, and M. C. Thompson, "On the flow past and forces on double-stacked wagons within a freight train under cross-wind," *Journal of Wind Engineering and Industrial Aerodynamics*, vol. 206, Nov. 2020, doi: 10.1016/j.jweia.2020.104224.
[15] S. Giappino, S. Melzi, and G. Tomasini, "High-speed freight trains for intermodal transportation: Wind tunnel study on the aerodynamic coefficients of container wagons," *Journal of Wind Engineering and Industrial Aerodynamics*, vol. 175, pp. 111–119, Apr. 2018, doi: 10.1016/j.jweia.2018.01.047.
[16] S. Giappino, D. Rocchi, P. Schito, and G. Tomasini, "Cross wind and rollover risk on lightweight railway vehicles," *Journal of Wind Engineering and Industrial Aerodynamics*, vol. 153, pp. 106–112, Jun. 2016, doi: 10.1016/j.jweia.2016.03.013.
[17] V. A. Golovanevskiy, V. V. Chmovzh, and Y. V. Girka, "On the optimal model configuration for aerodynamic modeling of open cargo railway train," *Journal of Wind Engineering and Industrial Aerodynamics*, vol. 107–108, pp. 131–139, 2012, doi: 10.1016/j.jweia.2012.03.035.
[18] A. Quazi, T. Crouch, J. Bell, T. McGreevy, M. C. Thompson, and D. Burton, "A field study on the aerodynamics of freight trains with different stacking configurations," *Journal of Wind Engineering and Industrial Aerodynamics*, vol. 232, Jan. 2023, doi: 10.1016/j.jweia.2022.105245.
[19] S. Maleki, D. Burton, and M. C. Thompson, "Assessment of various turbulence models (ELES, SAS, URANS and RANS) for predicting the aerodynamics of freight train container wagons," *Journal of Wind Engineering and Industrial Aerodynamics*, vol. 170, pp. 68–80, Nov. 2017, doi: 10.1016/j.jweia.2017.07.008.
[20] L. Corniani, P. Schito, and S. Bruni, "A4R-Freight-Train-Model-Geometries." Accessed: Sep. 08, 2025. [Online]. Available: https://github.com/lCornianiPolimi/A4R-Freight-Train-Model-Geometries

[21] L. Corniani, P. Schito, and S. Bruni, “Aerodynamics of Freight Trains: An Open Database of Geometries for CFD Analyses,” in *Proceedings of the Sixth International Conference on Railway Technology: Research, Development and Maintenance*, J. Pombo, Ed., Edinburgh: Civil-Comp Press, Sep. 2024. doi: 10.4203/ccc.7.3.20.